ISSN No: 2348-4845
International Journal & Magazine of Engineering, Technology, Management and Research
A Peer Reviewed Open Access International Journal

Direct Control Scheme for IPM Synchronous Generator with Gearless Wind Turbine

Cheerala Sreenivasulu
M.Tech Student
Department of EEE
P.V.K.K Institute of Technology.

M.Tasleema, M.Tech.
Guide
Department of EEE
P.V.K.K Institute of Technology.

G.N.S.Vaibhav, M.Tech.
HoD
Department of EEE
P.V.K.K Institute of Technology.

Abstract:

A wind turbine is a device that converts kinetic energy from the wind into electrical power. The term appears to have migrated from parallel hydroelectric technology. The technical description for this type of machine is an aerofoil-powered generator.

The result of over a millennium of windmill development and modern engineering, today's wind turbines are manufactured in a wide range of vertical and horizontal axis types. The smallest turbines are used for applications such as battery charging for auxiliary power for boats or caravans or to power traffic warning signs. Slightly larger turbines can be used for making contributions to a domestic power supply while selling unused power back to the utility supplier via the electrical grid. Arrays of large turbines, known as wind farms, are becoming an increasingly important source of renewable energy and are used by many countries as part of a strategy to reduce their reliance on fossil fuels.

In this scheme, the requirement of the continuous rotorpositionis eliminatedas all the calculationsaredonein the stator reference frame. This scheme possesses advantages such as lesser parameter dependence and reduced number of controllers compared with the traditional indirect vector control scheme.The direct control scheme is simpler and can eliminate some of the drawbacks of traditional indirect vector control scheme. The proposed control scheme is implemented in MATLAB/SimPowerSystems and the results show that the controller can operate under constant and varying wind speeds. Finally, a sensorless speed estimator is implemented, which enables the wind turbine to operate without the mechanical speed sensor. The simulation and experimental results for the sensorless speed estimator are presented.

*Index Terms—**Direct control, interior permanent magnet (IPM) synchronous generator, sensorless speed estimator, variable speed wind turbine.***

INTRODUCTION

The wind energy will play a major role to meet the renewable energy target worldwide, to reduce the dependency on fossil fuel, and to minimize the impact of climate change. Currently, variable speed wind turbine technologies dominate the world market share due to their advantages over fixed speed generation such as increased energy capture, operation at maximum power point, improved efficiency, and power quality. Most of these wind turbines use doubly fed induction generator (DFIG) based variable speed wind turbines with gearbox. This technology has an advantage of having power electronic converter with reduced power rating (30% of full rated power) as the converter is connected to the rotor circuit. However, the use of gearbox in these turbines to couple the generator with the turbine causes problems. Moreover, the gearbox requires regular maintenance as it suffers from faults and malfunctions.

Variable speed wind turbine using permanent magnet synchronous generator (PMSG) without gearbox can enhance the performance of the wind energy conversion system. The use of permanent magnet in the rotor of the PMSG makes it unnecessary to supply magnetizing current through the stator for constant air-gap flux. Therefore, it can operate at higher power factor and efficiency. The previous works done on

ISSN No: 2348-4845
International Journal & Magazine of Engineering, Technology, Management and Research
A Peer Reviewed Open Access International Journal

PMSG based wind turbines are mostly based on surface permanent magnet-type synchronous generator. Very few works have been done so far on interior PMSG-based wind turbines, which can produce additional power by exploiting their rotor saliency. It can also be operated over a wide speed range (more than rated speed) by flux weakening, which will allow constant power-like operation at speeds higher than the rated speed. This work is based on interior permanent magnet-type synchronous generator-based variable speed wind turbine.

There are different control strategies reported in the literature for permanent synchronous generator-based variable speed wind turbine such as switch-mode boost rectifier (uncontrolled diode rectifier cascaded by a boost dc–dc chopper, three-switch pulse width modulation (PWM) rectifier, and six-switch Vector-controlled PWM rectifier. The control of PMSG-based variable speed wind turbine with switch-mode rectifier has the merit of simple structure and low cost because of only one controllable switch. However, it lacks the ability to control generator power factor and introduces high harmonic distortion, which affects the generator efficiency. Moreover, this scheme introduces high voltage surge on the generator winding which can reduce the life span of the generator.

Traditional vector control scheme, as shown in Fig. (1) Is widely used in modern PMSG-based variable speed wind energy conversion system. In this scheme, the generator torque is controlled indirectly through current control. The output of the speed controller generates the - and –axes current references, which are in the rotor reference frame. The generator developed torque is controlled by regulating the currents and according to the generator torque equation. For high performance, the current control is normally executed at the rotor reference frame, which rotates with the rotor. Therefore, coordinate transformation is involved and a position sensor is, thus, mandatory for the torque loop. All these tasks introduce delays in the system. Also, the torque response under this type of control is limited by the time constant of stator windings. In this project, a direct control strategy is implemented where coordinate transformations are not required as all the calculations are done in stator reference frame. Thus, the requirement of continuous rotor position is eliminated.

This method is inherently sensorless and have several advantages compared with the traditional indirect vector control scheme. However, a speed sensor is required only for speed control loop. Therefore, a sensorless speed estimator is proposed and implemented in this paper to estimate the speed without a mechanical sensor.

WIND SYSTEMS

GRID-connected wind electricity generation is showing the highest rate of growth of any form of electricity generation, achieving global annual growth rates in the order of 20 - 25%. It is doubtful whether any other energy technology is growing, or has grown, at such a rate. Global installed capacity was 47.6 GW in the year 2004 and 58.9 GW in 2005. Wind power is increasingly being viewed as a mainstream electricity supply technology. Its attraction as an electricity supply source has fostered ambitious targets for wind power in many countries around the world. Wind power penetration levels have increased in electricity supply systems in a few countries in recent years; so have concerns about how to incorporate this significant amount of intermittent, uncontrolled and non-dispatchable generation without disrupting the finely-tuned balance that network systems demand. Grid integration issues are a challenge to the expansion of wind power in some countries. Measures such as aggregation of wind turbines, load and wind forecasting and simulation studies are expected to facilitate larger grid penetration of wind power.

In this project simulation studies on grid connected wind electric generators (WEG) employing (i) Squirrel Cage Induction Generator (SCIG) and (ii) Doubly Fed Induction Generator (DFIG) have been carried separately. Their dynamic responses to disturbances such as variations in wind speed, occurrence of fault

ISSN No: 2348-4845
International Journal & Magazine of Engineering, Technology, Management and Research
A Peer Reviewed Open Access International Journal

etc. have been studied, separately for each type of WEG.

Power from Wind

The power that can be captured from the wind with a wind energy converter with effective area Arc is given by

$$P = \frac{1}{2}\rho_{air} C_p A v_w^3$$

Where pair is the air mass density [kg/m3], vw is the wind speed and Cp is the so-called power coefficient which depends on the specific design of the wind converter and its orientation to the wind direction. Its theoretical maximum value is 16/27 = 0.593 (Betz limit). For a wind turbine with given blades it can be shown that the power coefficient Cp basically depends only on the tip speed ratio l, which equals the ratio of tip speed vt [m/s] over wind speed vw [m/s] and the so-called blade pitch angle q [deg]. This pitch angle is defined as the angle between the cord of the blade and the plane of the wind rotor. So, for a wind rotor with radius r , can be rewritten as:

$$P = \frac{1}{2}\rho_{air} C_p(\lambda,\theta)\pi r^2 v_w^3$$

As an example, Fig. 2 shows the dependency of the power coefficient Cp on the tip speed ratio l and the blade pitch angle q for a specific blade. For this blade maximum energy capture from the wind is obtained for q =0 and l just above 6. To keep Cp at its optimal value for varying wind speed, the rotor speed should be proportional to the wind speed. In practice both constant l (variable speed) and constant speed operation is applied.

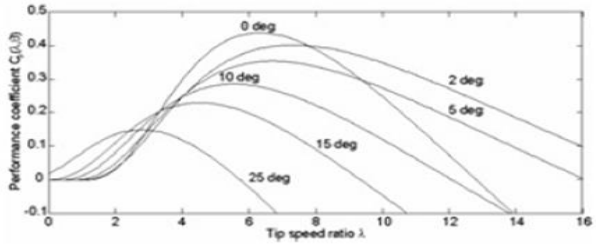

Fig 1: Power coefficient Cp as a function of tip speed ratio l and pitch angle q for a specific blade.

For on shore turbines, the blades are designed such that the optimal tip speed is limited to roughly 70 m/s. This is done because the blade tips cause excessive acoustical noise at higher tip speeds. For offshore turbines, the noise does not play an important role, and higher speeds are used leading to slightly higher optimal values of Cp. The relation between wind speed and generated power is given by the power curve, as depicted. The power curve can be calculated from where the appropriate value of l and q should be applied. In the power curve, four operating regions can be distinguished, that apply both to constant speed and variable speed turbines:

1. No power generation due to the low energy content of the wind.
2. Less than rated power generation. In this region, optimal aerodynamic efficiency and energy capture is aimed at. The wind speed at the boundary of region 2 and 3 is called the rated wind speed and all variables with the subscript rated refer to design values at this wind speed.
3. Generation of rated power, because the energy content of the wind is enough. In this region, the aerodynamic efficiency must be reduced, because otherwise the electrical system would become overloaded.
4. No power generation. Because of high wind speeds the turbine is closed down to prevent damage.

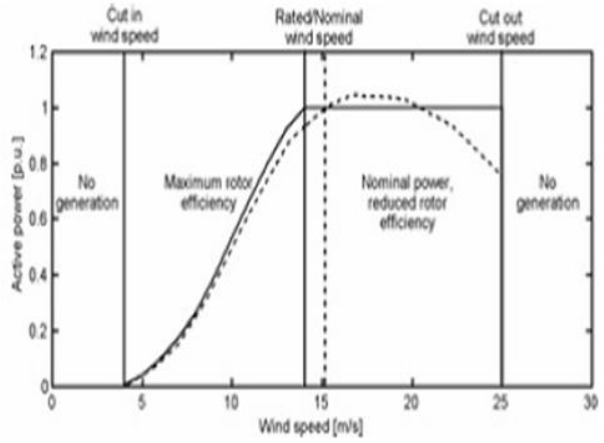

Fig 2: Typical power curve of a constant speed stall (dotted) and a variable speed pitch (solid) controlled wind turbine.

ISSN No: 2348-4845
International Journal & Magazine of Engineering, Technology, Management and Research
A Peer Reviewed Open Access International Journal

Aerodynamic Power control

In region 3 and 4 the shaft power should be less than the available power from wind to prevent overloading of components. There are two main methods for limiting the aerodynamic efficiency in high wind speeds. With the first method one takes advantage of the aerodynamic stall effect. When the angle, at which the wind hits the blade (‘angle of attack’), is gradually increased, then at a certain angle the airflow will no longer flow along the blade, but will become loose from the blade at the back side. Large eddy’s will be formed that result in a drastic reduction of Cp (see Fig. 3).

If a turbine is operated at constant speed and the wind speed increases, then automatically the angle of attack increases. At a certain wind speed the angle of attack will reach the value where stall occurs. Here it is assumed that the pitch angle q is not changed. With so-called stall controlled turbines the blade are designed such that the stall effect just starts at the rated wind speed. Due to the stall effect, the power is more or less constant above rated wind speed, as indicated by the dotted curve in active control systems are used to achieve this, which also implies that the blade does not need to be patchable. With variable speed (constant l) wind turbines the angle of attack is independent of the wind speed so that the stall effect does not occur. To reduce the power above the rated wind speed the blades are pitched towards the vane position by hydraulic or electric actuators resulting in a reduction of Cp.

Above the rated wind speed the variable speed turbines are normally operated at constant speed, where power (so torque) is controlled by the pitch angle. This result in a flat power curve above the rated wind speed From above it will be obvious that stall control is mainly used with constant speed turbines and pitch control with variable speed wind turbines.

$$E = \int_0^\infty P(v_w) \cdot u(v_w) dv_w$$

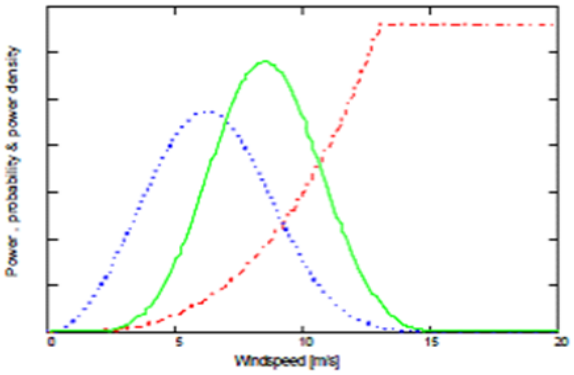

The annual energy yield E of a wind turbine depends on its power curve P(vw) and the probability density distribution function u(vw) of the wind speed at the turbine site: Power P (red, dashed), probability density U (blue, dotted) and power density (green, solid) as a function of wind speed (arbitrary units).

Scaling laws

As stated before the rated tip speed should be limited to about 70 m/s. If the same rated tip speed vtrated is assumed independent of the size of the wind rotor, then the rotational speed of the rotor is inversely proportional to radius of the wind rotor. With (2) this results in:

$$N_{rated} = \frac{60}{2\pi} \frac{v_{trated}}{r} \propto \frac{1}{\sqrt{P_{rated}}}$$

Where v rated is the rated tip speed. For the torque this implies that:

$$T_{rated} = \frac{P_{rated}}{\omega_{rated}} \propto P_{rated}^{3/2}$$

The size of the generator is related to the torque to be developed. The force density (the force per square metre of active air gap surface area) in electrical machines is a quantity that is rather constant over a wide range of machine powers. For the conventional generators used in wind turbines, the air gap force density is in the order of

$$F_d = 25 - 50 \text{ kN/m}^2$$

ISSN No: 2348-4845
International Journal & Magazine of Engineering, Technology, Management and Research
A Peer Reviewed Open Access International Journal

This force density is rather constant because it is the product of air gap flux density, which is limited because of magnetic saturation, and current loading, which is limited because of dissipation. By using forced liquid cooling, this force density can be increased, but at the cost of reduced efficiency. Based on this force density, a very fast and rather good estimate of the generator dimensions can be made. The torque produced by a machine is given by

$$P = \omega T = \omega r_s F_d = 2\omega\pi r_s^2 l_s F_d$$

Where w is the mechanical angular frequency, rs is the stator bore radius, and ls is the stator stack length. From this, the rotor volume of a generator can be estimated as

$$V_r = \pi r_s^2 l_s = \frac{P}{2\omega F_d}$$

If we further assume that the rated tip speed is independent from rated power, then for direct-drive wind turbines according to this reduces to:

$$V_r \propto \frac{P_{rated}^{3/2}}{2F_d}$$

ELECTRICAL SYSTEM

Currently used Generator Systems

As stated before two types of wind turbines can be distinguished namely variable speed and constant speed turbines. For constant speed turbines one applies induction generators that are directly connected to the grid. For variable speed turbines a variety of conversions systems is available. The three most commonly used generator systems applied in wind turbines are depicted in figure 4 and discussed below.

a) Constant speed wind turbine with squirrel cage induction generator (CT)

b) Variable speed wind turbine with doubly-fed (wound rotor) induction generator (VTDI)

c) Variable speed wind turbines with direct-drive synchronous generator (VTDD)

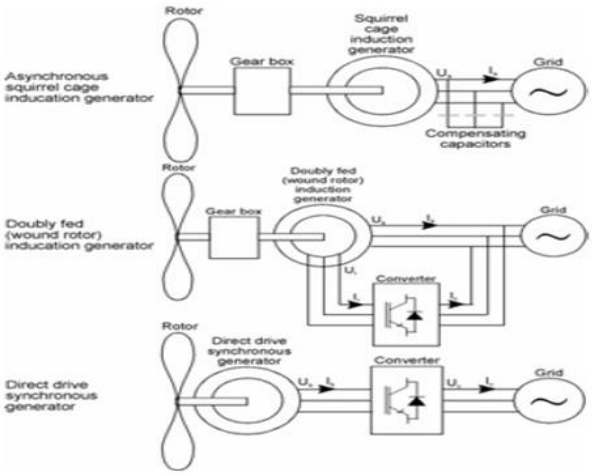

Fig. 3: The three commonly used generator systems.

Constant speed wind turbine with squirrel cage induction generator (CT):

Between the rotor and the generator, there is a gearbox so that a standard (mostly 1500 rpm) squirrel cage induction generator can be used. The generator is directly connected to the 50 Hz or 60 Hz utility grid. Mostly, the power is limited using the classic stall principle: if the wind speed increases above the rated wind speed, the power coefficient inherently reduces, so that the power produced by the turbine stays near the rated power. Sometimes active stall is used: negative pitch angles are used to limit the power. There are a few variants:

1 pole changing generators with two stator windings with different numbers of pole pairs so that the turbine can operate at two constant speeds in order to increase energy yield and reduce audible noise, and

2 generators with electronically variable rotor resistance in order to reduce mechanical loads by making larger speed variations possible: the semi variable speed wind turbine.

Variable speed wind turbine with doubly-fed (wound rotor) induction generator (VTDI)

Between the rotor and the generator, there is a gearbox so that a standard (mostly 1500 rpm) doubly-fed

ISSN No: 2348-4845
International Journal & Magazine of Engineering, Technology, Management and Research
A Peer Reviewed Open Access International Journal

induction generator can be used. The stator is directly connected to the utility grid. The rotor is connected to a converter. A speed range from roughly 60% to 110 % of the rated speed is sufficient for a good energy yield, that is achieved by using the variable speed capability to keep the tip speed ratio l at the value resulting in optimal energy capture. If the gearbox ratio is chosen such that the synchronous speed of the generator just falls in the middle of the speed range (in this case at 85% of rated speed), then the lowest converter power rating is obtained.

A converter rating of roughly 35 % of the rated turbine power is sufficient, particularly when star-delta switching at the rotor winding is applied. At wind speeds above the rated wind speed, the power is reduced by pitching the blades.

Variable speed wind turbines with direct-drive synchronous generator (VTDD)

In this system, no gearbox is necessary, because the generator rotates at very low speed, typically 10 to 25 rpm for turbines in the MW range. Standard generators can therefore not be used and generators have to be developed specifically for this application. As can be concluded from equations and these generators are very large because they have to produce a huge torque. The total turbine power goes through a converter that converts the varying generator frequency to the constant grid frequency. At wind speeds above the rated wind speed, the power is again reduced by pitching the blades.

Comparison of the three systems

		CS	VTDI	VTDD
Cost, size and weight		+	+/-	-
Suitability for 50 and 60 Hz grid frequency		-	-	+
Audible noise from blades		-	+	+
Energy yield	Variable speed	-	+	+
	Gearbox	-	-	+
	Generator	+	+	-
	Converter	+	+/-	-
Reliability and Maintenance	Brushes	+	-	- (PM:+)
	Gearbox	-	-	+
	Mechanical loads	-	+	+
	Complexity	+	-	-
Power quality	'Flicker'	-	+	+
	Grid V&f control possible	-	+	+
	Harmonics	+	-	-
Grid faults	Fault currents	+	+	+/-
	Restoring voltage	-	+	+

Table - 1 Comparison of the Three Systems.

Cost, size and weight

Squirrel cage induction generators are roughly 25% cheaper than doubly-fed (wound-rotor) induction generators. The converter for a doubly-fed induction machine is smaller and cheaper than for a direct-drive generator. Direct-drive generators are much more expensive because they are large and heavy and have to be specially developed. However, direct drive turbines do not need a heavy gearbox.

Suitability for 50 and 60 Hz grid frequency

Turbines wit h generators that are directly coupled to the grid (CT and VTDI) need different gearboxes for different grid frequencies. This is not the case when a converter decouples the two frequencies.

Audible noise from blades

In a well-designed wind turbine, the blades are the main sources of audible noise. In variable speed wind turbines, the rotor speed is low at low wind speeds, and so is the audible noise. This is not the case in constant speed wind turbines. At higher wind speed the noise from the blade tips drowns in the wind noise caused by obstacles more close to the observer. However, in a wind turbine that is not properly designed, mechanical resonance can also cause other audible noise.

Energy yield

In order to capture the maximum energy from the wind, the rotor speed has to be proportional to the wind speed in region 2 of figure 3. Therefore, the energy yield of variable speed wind turbines is larger than of constant speed wind turbines. Especially in part load, gearboxes and power electronic converters have limited efficiencies. Direct-drive generators have lower efficiencies than standard induction machines.

Reliability and maintenance

Brushed synchronous generators and doubly-fed induction generators have brushes, which need regular inspection and replacement. Permanent magnet (PM) and squirrel cage induction generators don't have this problem. Gearboxes are widely used, well-known

ISSN No: 2348-4845
International Journal & Magazine of Engineering, Technology, Management and Research
A Peer Reviewed Open Access International Journal

components with many of applications. However, in wind turbines, gearboxes show a reliability record that is rather negative. In constant speed wind turbines, wind gusts immediately lead to torque variations, while in variable speed wind turbines, wind gusts lead to variations in the speed without large torque variations. Therefore, constant speed wind turbines suffer from heavier mechanical loads, which may result a decrease in reliability and an increase in maintenance. Generally, more complex systems suffer from more failures than simple systems.

Power quality

It depicts measurements of wind speed sequences and the resulting rotor speeds, pitch angles and output powers for the three most used generator systems at wind speeds around the rated wind speed. It appears that the power output of variable speed wind turbines is much smoother (less 'flicker') than constant speed wind turbines because rapid changes in the power drawn from the wind are buffered in rotor inertia. The fast power fluctuations in constant speed wind turbines are caused by variations in wind speed, but also by the tower shadow. If the converter rating is large enough, variable speed wind turbines also can be used for voltage and frequency (V&f) control in the grid (within the limits posed by the actual wind speed), which is not possible with constant speed wind turbines. Power electronic converters produce harmonics that may need to be filtered away.

Grid faults

The three concepts behave differently in case of a grid fault causing a voltage dip. In case of a fault, constant speed wind turbines can deliver the large fault currents, necessary for activating the protection system. However, when the voltage comes back, they consume a lot of reactive power and thus impede the voltage restoration after the dip. In addition both the fault and the reconnection results in large torque excursions that may damage the gear box.

IPM SYNCHRONOUS GENERATOR MODEL

The machine model in reference frame, which is synchronously rotating with the rotor, where -axis is aligned with the magnet axis and -axis is orthogonal to -axis, is usually used for analyzing the interior permanent magnet (IPM) synchronous machine [23]. The - and -axes voltages of PMSG can be given by

$$v_d = -i_d R_s - \omega_r \lambda_q + p\lambda_d \quad (7)$$

$$v_q = -i_q R_s + \omega_r \lambda_d + p\lambda_q. \quad (8)$$

The d- and q-axesflux linkages are given by

$$\lambda_d = -L_d i_d + \lambda_M \quad (9)$$

$$\lambda_q = -L_q i_q. \quad (10)$$

The torque equation of the PMSG can be written as

$$T_g = -\frac{3}{2}P(\lambda_d i_q - \lambda_q i_d) = -\frac{3}{2}P[\lambda_M i_q + (L_d - L_q) i_d i_q]. \quad (11)$$

In (7)–(11), The stator voltages, currents, and inductances, respectively, is the stator resistance, is the rotor speed in red/s, is the magnet flux, is the number of pole pairs, and is the operator . Fig. 6 shows the model of IPM synchronous generator.

The first term in the torque equation (11) is the excitation torque that is produced by the interaction of permanent magnet flux and is independent of The second term is the reluctance torque that is proportional to the product of and to the difference between them. For the surface PMSG, the reluctance torque is zero since, while for the IPM synchronous generator, higher torque can be induced for the same and, if it is larger.

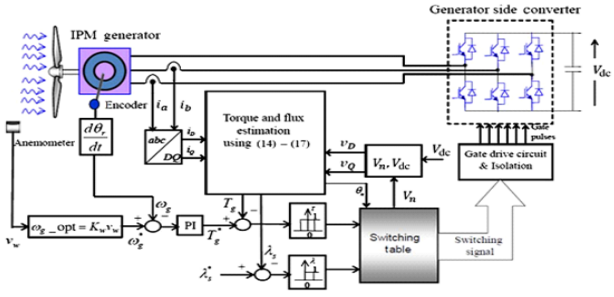

Fig 5: Proposed direct control scheme for the IPM generator side converter

ISSN No: 2348-4845
International Journal & Magazine of Engineering, Technology, Management and Research
A Peer Reviewed Open Access International Journal

This is one of the advantages of IPM synchronous generator over surface PMSG. The current References can be shown as or by given below equations,

$$i_q^* = \frac{2T_g^*}{3P[\lambda_M + (L_d - L_q)]i_d} \quad (12)$$

$$i_d^* = \frac{\lambda_M}{2(L_d - L_q)} - \sqrt{\frac{\lambda_M^2}{4(L_d - L_q)} + (i_q^*)^2}. \quad (13)$$

PROPOSED DIRECT CONTROL SCHEME FOR IPM SYNCHRONOUS GENERATOR

The direct control scheme for IPM synchronous generator is shown in Fig.5. In this scheme, current controllers are not used. Instead, the flux linkage and torque are controlled directly. The torque and flux are controlled using two hysteresis controllers

θ		θ_1	θ_2	θ_3	θ_4	θ_5	θ_6
λ	τ						
λ=1	τ=1	$V_{2(110)}$	$V_{3(010)}$	$V_{4(011)}$	$V_{5(001)}$	$V_{6(101)}$	$V_{1(100)}$
	τ=0	$V_{6(101)}$	$V_{1(100)}$	$V_{2(110)}$	$V_{3(010)}$	$V_{4(011)}$	$V_{5(001)}$
λ =0	τ=1	$V_{3(010)}$	$V_{4(011)}$	$V_{5(001)}$	$V_{6(101)}$	$V_{1(100)}$	$V_{2(110)}$
	τ=0	$V_{5(001)}$	$V_{6(101)}$	$V_{1(100)}$	$V_{2(110)}$	$V_{3(010)}$	$V_{4(011)}$

Table II: - Six-Vector Switching Table for Converter

And by selecting optimum converter switching modes, as shown in Fig. 4. The selection rule is made to restrict the torque and flux linkage errors within the respective torque and flux hysteresis bands to achieve the desired torque response and flux linkage. The required switching-voltage vectors can be selected by using a switching-voltage vector lookup table, as shown in Table II.

The selection of the voltage space vectors can be determined by the position of the stator flux linkage vector and the outputs of the two hysteresis comparators. The hysteresis control blocks compare the torque and flux references with estimated torque and flux, respectively. When the estimated torque/flux drops below its differential hysteresis limit, the torque/flux status output goes high. When the estimated torque/ flux rises above differential hysteresis limit, the torque/flux output goes low. The differential limits, switching points for both torque and flux, are determined by the hysteresis bandwidth.

The appropriate stator voltage vector can be selected by using the switching logic to satisfy both the torque and flux status outputs. There are six voltage vectors and two zero voltage vectors that a voltage source converter can produce. The combination of the hysteresis control block (torque and flux comparators) and the switching logic block eliminates the need for a traditional PW modulator. The optimal switching logic is based on the mathematical spatial relationships of stator flux, rotor flux, stator current, and stator voltage. These relationships are shown in Fig. 5 as rotor flux reference, stator flux reference, and stationary reference frames. The angle between the stator and rotor flux linkages is the load angle if the stator resistance is neglected. In the steady state, is constant corresponding to a load torque and both stator and rotor fluxes rotate at the synchronous speed. In the transient operation, varies and the stator and rotor fluxes rotate at different speeds. The magnitude of the stator flux is normally kept as constant as possible, and the torque is controlled by varying the angle between the stator flux vector and the rotor flux vector. In direct torque and flux control scheme, the stator flux linkage is estimated by integrating the difference between the input voltage and the voltage drop across the stator resistance, as given by

$$\lambda_D = -\int (v_D - i_D R_s)dt \quad (14)$$

$$\lambda_Q = -\int (v_Q - i_Q R)dt. \quad (15)$$

ISSN No: 2348-4845
International Journal & Magazine of Engineering, Technology, Management and Research
A Peer Reviewed Open Access International Journal

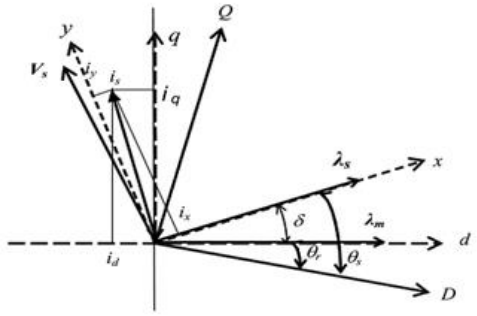

Fig 6: Stator and rotor flux linkages in different reference frame

In the stationary reference frame, the stator flux linkage phasor is given by

$$|\boldsymbol{\lambda}_s| = \sqrt{\lambda_D^2 + \lambda_Q^2} \quad \text{and} \quad \angle\theta_s = \tan^{-1}(\lambda_Q/\lambda_D) \qquad (16)$$

And the electromagnetic torque is given by

$$T_g = -\frac{3}{2}P(\lambda_D i_Q - \lambda_Q i_D). \qquad (17)$$

The torque equation in terms of and generator parameters is given by

$$T_g = -\frac{3P|\boldsymbol{\lambda}_s|}{4L_d L_q}(2\lambda_M L_q \sin\delta - |\boldsymbol{\lambda}_s|(L_q - L_d)\sin 2\delta). \qquad (18)$$

CONTROL OF STATOR FLUX LINKAGE BY SELECTING PROPER STATOR VOLTAGE VECTOR

The stator voltage vector for a three-phase machine with balanced sinusoidally distributed stator windings is defined by the following equation:

$$\mathbf{v}_s = \frac{2}{3}(v_a + v_b e^{j2\pi/3} + v_c e^{j4\pi/3})$$

Where the phase“ ”axis is taken as the reference position and , are the instantaneous values of line to neutral voltages. In Fig. 7, the ideal bidirectional switches represent the power Switches with their anti parallel diodes. The primary voltages, and are determined by the status of these three switches.

Therefore, there are six nonzero voltage vectors, two zero voltage vectors. The six nonzero voltage vectors are 60 apart from each other, as in Fig. 8. These eight voltage vectors can be expressed as

$$\mathbf{v}_s(S_a, S_b, S_c) = V_D(S_a + S_b e^{j2\pi/3} + S_c e^{j4\pi/3})$$

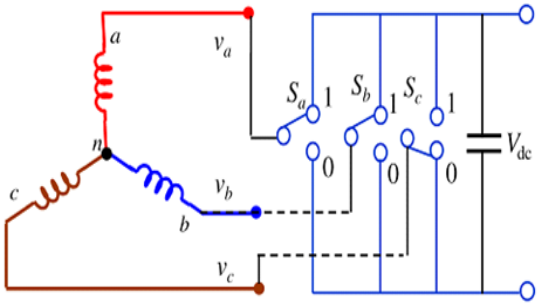

Fig 7: Rectifier connected to IPM synchronous generator

where $V_D = 2/3V_{dc}$ and V_{dc} = dc-link voltage.

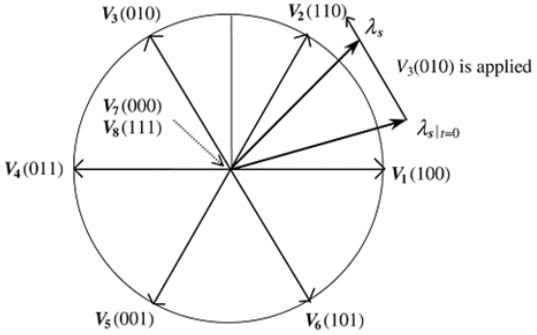

Fig 8: Available stator voltage vectors

A. Control of Amplitude of Stator Flux Linkage The statorflux linkage in the stationary reference frame can be given as

$$\boldsymbol{\lambda}_s = \int (\mathbf{v}_s - i_s R_s)dt.$$

The above Equation can be written as

$$\boldsymbol{\lambda}_s = \mathbf{v}_s t - R_s \int i_s dt.$$

ISSN No: 2348-4845
International Journal & Magazine of Engineering, Technology, Management and Research
A Peer Reviewed Open Access International Journal

The above equation implies that the tip of the stator flux linkage vector will move in the direction of the applied voltage vector if the stator resistance is neglected, as shown in Fig. 8. How far the tip of the stator flux linkage will move is determined by the duration of time for which the stator vector is applied. In Fig. 9, the voltage vector plane is divided into six regions – to select the voltage vectors for controlling the amplitude of the stator flux linkage. In each region, two adjacent voltage vectors are selected to keep the switching frequency minimum. Two voltages may be selected to increase or decrease the amplitude of. For instance, voltage vectors and are selected to increase or decrease the amplitude of, respectively, when is in region and the stator flux vector is rotating in counter clockwise direction.

In this way, the amplitude of can be controlled at the required value by selecting the proper voltage vectors. How the voltage vectors are selected for keeping within a hysteresis band is shown in Fig. 9 for a counter clockwise direction of. The hysteresis band here is the difference in radii of the two circles in Fig. 9.

To reverse the rotational direction of, voltage vectors in the opposite direction should be selected. For example, when is in region and is rotating in the clockwise direction

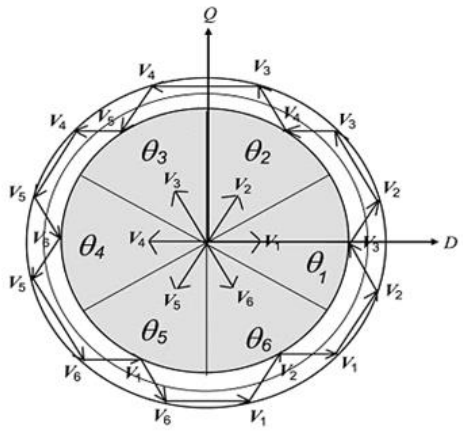

Fig 9: Control of the amplitude of stator flux linkage

The voltage vectors pair and are selected to reverse the Control of Rotation. The effect of two nonzero voltage vectors and is more complicated. It is seen that it will stay at its original position when zero voltage vectors are applied. This is true for induction machine since the stator flux linkage is uniquely determined by the stator voltage, where the rotor voltages are always zero. In the case of an IPM synchronous generator, will change even when the zero voltage vectors are applied, since magnet flux continues to be supplied by the rotor and it will rotate with the rotor. In other words, should always be in motion with respect to the rotor flux linkage. Therefore, zero voltage vectors are not used for controlling in IPM synchronous machine.

The electromagnetic torque is controlled by controlling the direction of rotation of, according to the torque equation. For counter clockwise operation, if the actual torque is smaller than the reference value, the voltage vectors that keep rotating in the same direction are selected. The angle increases as fast as it can and the actual torque increases as well.

Once the actual torque is greater than the reference value, the voltage vectors that keep rotating in the reverse direction are selected instead of the zero voltage vectors. The angle decreases and torque decreases too. By selecting the voltage vectors in this way, is rotated all the time and its rotational direction is determined by the output of the hysteresis controller for the torque. The six-vector switching table for controlling both the amplitude and rotating direction of is shown in Table I and is used for both the directions of operations. In Table II, and are the outputs of the hysteresis controllers for flux linkage and torque, respectively. If, then the actual flux linkage is smaller than the reference value.

IMPLEMENTATION OF DIRECT CONTROLSCHEME FOR IPM SYNCHRONOUS GENERATOR-BASED WIND TURBINE

The direct control scheme for IPM synchronous generator is shown in Fig. 4, where the switching

ISSN No: 2348-4845
International Journal & Magazine of Engineering, Technology, Management and Research
A Peer Reviewed Open Access International Journal

scheme used is shown in Table II. The three-phase variables are transformed into stationary

	V_1	V_2	V_3	V_4	V_5	V_6
v_D	V_D	$0.5V_D$	$-0.5V_D$	$-V_D$	$-0.5V_D$	$0.5V_D$
v_Q	0	$0.886V_D$	$0.886V_D$	0	$-0.886V_D$	$-0.886V_D$

Table III: - DQ-Axes Voltages

Axes variables. As shown in Fig. 5, torque error and flux error are the inputs to the flux hysteresis comparator and torque hysteresis comparator, respectively. The outputs of the hysteresis comparators are the inputs to the voltage-switching selection lookup table. As shown in Fig. 5, this scheme is not dependent on generator parameters except the stator resistance. Moreover, all calculations are in the stator reference frame and without any co-ordinate transformation.

Flux Linkage and Torque Estimation

The axes flux linkage components and at the sampling instant can be calculated as

$$\lambda_{D(k)} = T_s[-v_{D(k-1)} + R_s i_{D(k)}] + \lambda_{D(k-1)}$$
$$\lambda_{Q(k)} = T_s[-v_{Q(k-1)} + R_s i_{Q(k)}] + \lambda_{Q(k-1)}$$

Where is the sampling time, the variables with subscript are their values at the sampling instant, and the variables with are the previous samples. The axes currents can be obtained from the measured three-phase currents and the -axes voltages are calculated from the measured dc-link voltages. Table III shows and axes voltages for the applied voltage vectors. The amplitude of the stator flux linkage is calculated from

$$|\boldsymbol{\lambda}_{s(k)}| = \sqrt{\lambda_{D(k)}^2 + \lambda_{Q(k)}^2} \text{ and } \theta_s = \angle\tan^{-1}(\lambda_{Q(k)}/\lambda_{D(k)}).$$

The developed torque is calculated from

$$T_{g(k)} = -\frac{3}{2}P(\lambda_{D(k)} i_{Q(k)} - \lambda_{Q(k)} i_{D(k)}).$$

The generator developed torque, in terms of stator and rotor flux linkage amplitudes, is also given by

$$T_{g(k)} = -\frac{3P|\boldsymbol{\lambda}_{s(k)}|}{4L_d L_q} \times [2\lambda_M L_q \sin\{\delta_{(k)}\} - |\boldsymbol{\lambda}_{s(k)}|(L_q - L_d)\sin 2(\delta_{(k)})].$$

SIMULATION AND RESULTS

The direct control scheme for IPM synchronous generator based variable speed wind turbine shown in Fig.5 is implemented in MATLAB/Sim Power Systems dynamic system simulation software. The IPM synchronous generator data are given in Table III. Table I is used for switching the converter. The bandwidths of torque and flux hysteresis controllers are 10% of their rated values.

Rated power	4.7 kW
Rated torque	34.8 Nm
Rated speed	1280/ 1600 rpm
Rated voltage	400/480 V rms
Rated current	8.1 A rms
Magnet flux linkage	0.525723 Wb
d-axis inductance (L_d) per phase	18.237 mH
q-axis inductance (L_q) per phase	49.239 mH
Stator resistance	1.56 Ω
No. of poles	6
Rotor inertia	0.0049 kg·m²
Static friction	0.637 N·m
Viscous damping	0.237 N·m/krpm

TABLE IV: - parameters of IPM Synchronous Generator

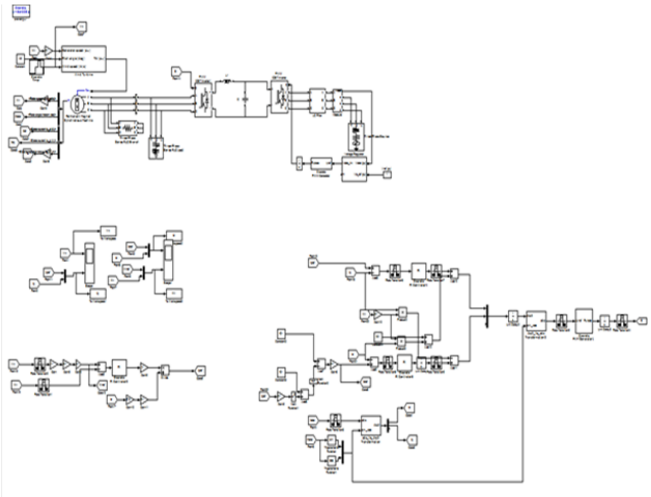

Fig: 19. Traditional indirect control scheme of IPM

ISSN No: 2348-4845
International Journal & Magazine of Engineering, Technology, Management and Research
A Peer Reviewed Open Access International Journal

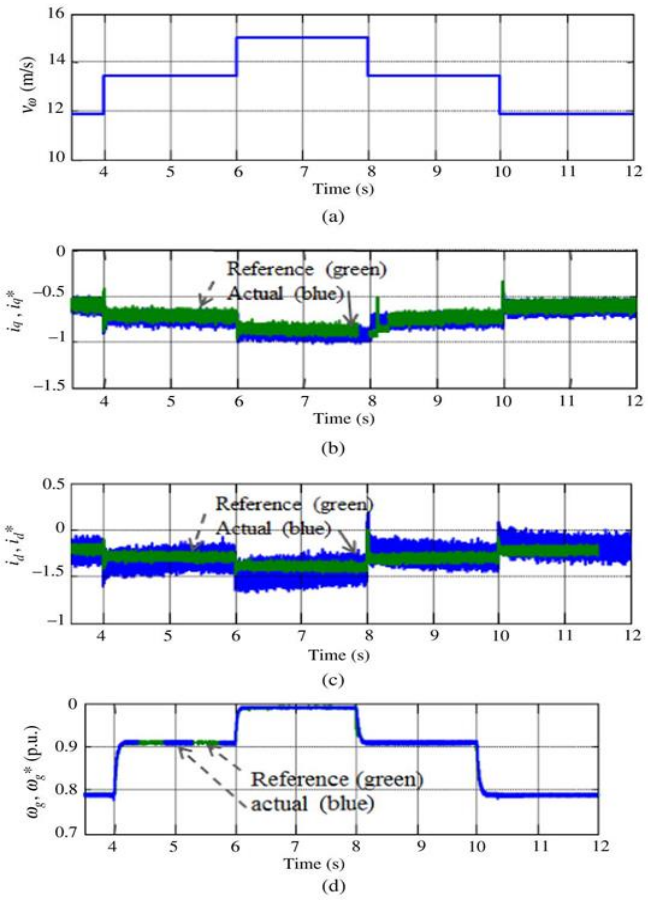

Fig 20. Simulation Results of the indirect vector control scheme.

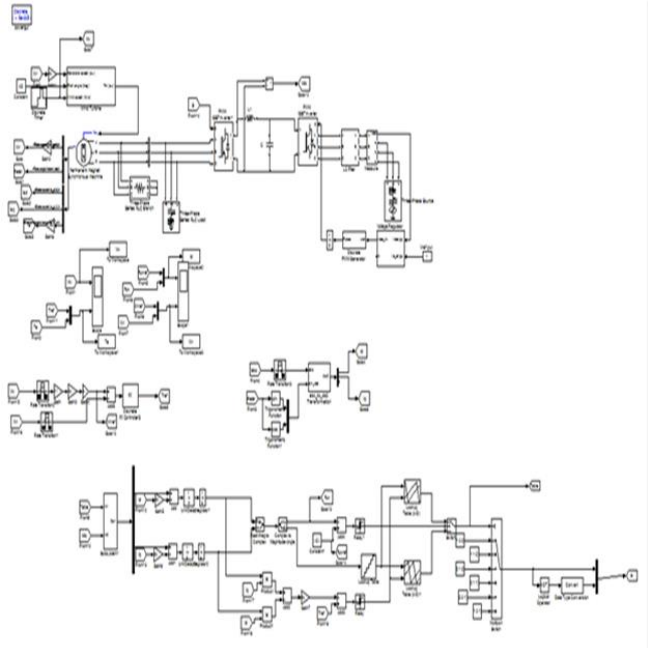

Fig:-21. Proposed direct vector control scheme

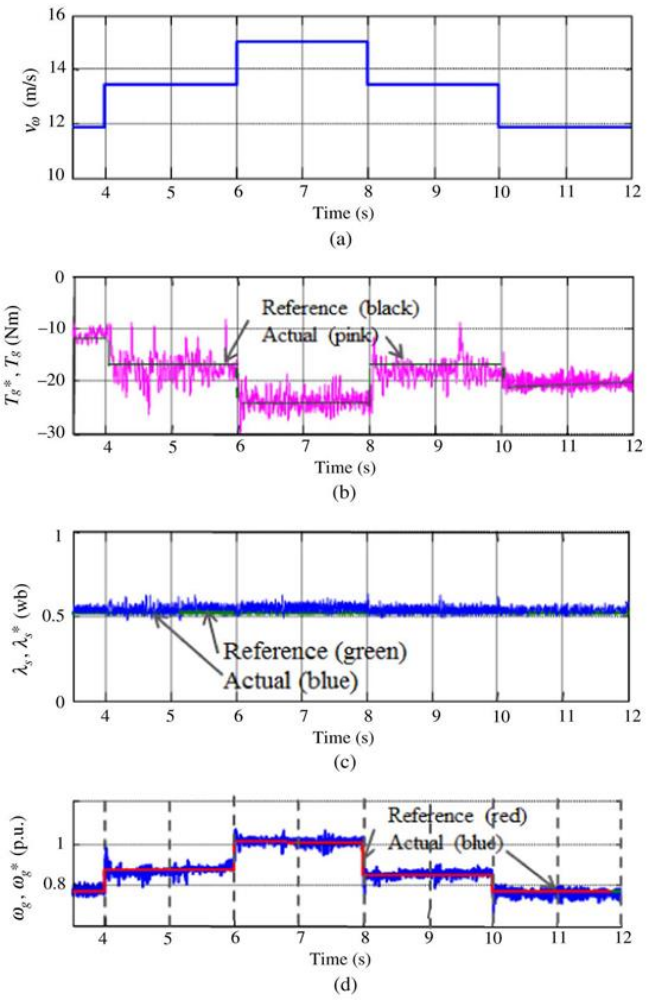

Fig. 22.Simulation Results of direct control scheme.

A smaller hysteresis bandwidth can reduce ripples in torque. The sampling times for the torque and speed control loops are 10 and, respectively. For comparison, the traditional vector-controlled scheme shown in Fig. (2) Has also been implemented in MATLAB/Sim Power Systems using the same IPM synchronous generator. MATLAB/Sim Power Systems wind turbine model is used in this work. The input to the wind turbine model is wind speed and the output is torque.

A. Performance of the Indirect Vector Control Scheme
Fig. 10 shows the performance of the indirect vector control of IPM synchronous generator-based variable speed wind turbine. The and axes currents and their references are shown in Fig. 10(b) and (c),

ISSN No: 2348-4845
International Journal & Magazine of Engineering, Technology, Management and Research
A Peer Reviewed Open Access International Journal

respectively, and the wind speed in Fig. 10(a). It is seen that and -axes currents follow their references quite well and regulate the generator current under different wind speeds. As shown in Fig. 10(d), the speed controller is able to regulate the speed for varying wind speeds.

B. Performance of Direct Torque and Flux Control Scheme Fig. (11) Shows the performance of direct control scheme for IPM synchronous generator-based variable speed wind turbine.

Fig. (11) (a)–(d) shows the wind speed, torque response, flux linkage response, and speed response, respectively. As shown in Fig. (11)(b) and (c), the torque and flux linkages are following these references quite well and regulate the torque and flux of the generator at different wind speeds. Fig. (11)(d) Shows the speed response, where the measured speed follows the reference speed well and the speed controller regulates the generator speed under varying wind conditions.

C. Maximum Power Extraction at Variable Wind Speed Figs. (12) And (13) show the maximum power extraction at different wind speeds under indirect vector control and direct torque and flux control scheme, respectively. In both control schemes, the measured power can track the optimum power curve quite well and extract the maximum power at different wind speeds.

The deviations between the measured and optimum values are within 2%.

D. Performance Comparison It is seen from Figs. (10) to (13) that direct torque and flux control scheme shows similar performance to indirect vector control scheme No rotor position is required with direct control scheme as all the calculations are done in stator reference frame.

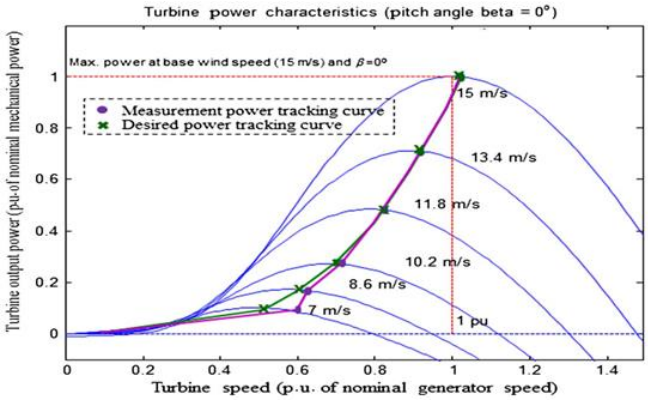

Fig 23. Maximum power extraction with indirect control scheme

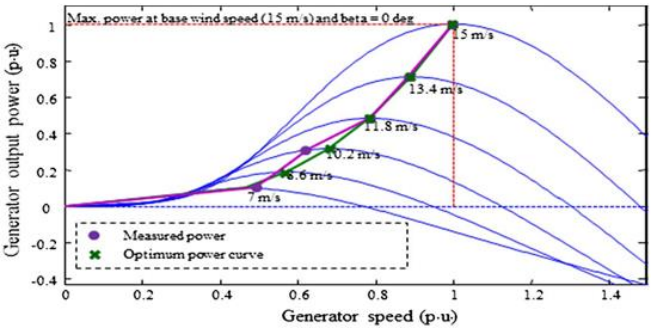

Fig 24. Maximum power extraction with direct control scheme

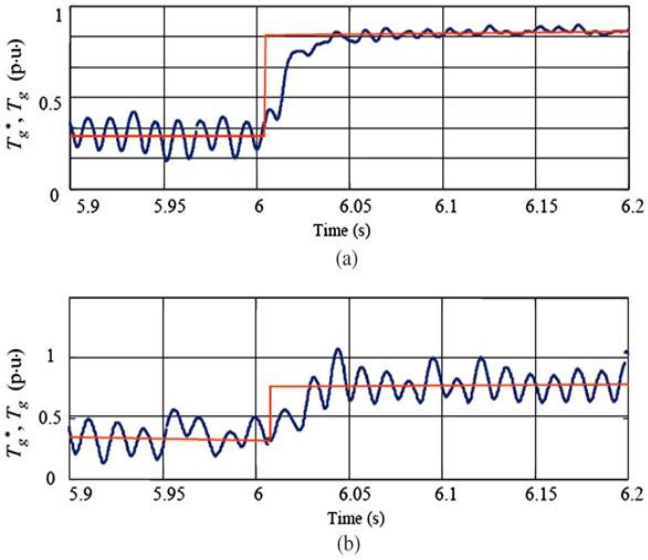

Fig 25. Comparison of Torque response (a) torque response under vector control scheme and (b) Torque response under direct control scheme.

ISSN No: 2348-4845
International Journal & Magazine of Engineering, Technology, Management and Research
A Peer Reviewed Open Access International Journal

CONCLUSION

This project proposed a sensorless direct control strategy for an IPM synchronous generator-based variable speed wind turbine. In this control scheme, no rotor position is required as all the calculations are done in stator reference frame. The proposed direct control scheme possesses several advantages compared with indirect vector control scheme, such as: 1) lesser parameter dependence; 2) torque and flux control without rotor position and PI controller which reduce the associated delay in the controllers; and 3) sensorless operation without mechanical sensor.

The results show that the direct controller can operate under varying wind speeds. However, direct control scheme has the problem of higher torque ripple that can introduce speed ripples and dynamic vibration in the power train. The methods to minimize the torque/ speed ripples need to be addressed. The simulation and experimental results for the sensorless speed estimator are presented, and the results show that the estimator can estimate the generator speed quite well with a very small error.

In this project simulation studies on grid connected wind electric generators (WEG) employing (i) Squirrel Cage Induction Generator (SCIG) and (ii) Doubly Fed Induction Generator (DFIG) have been carried separately. Their dynamic responses to disturbances such as variations in wind speed, occurrence of fault etc. have been studied, separately for each type of WEG.

REFERENCES

[1] S. Müller, M. Deicke, and R. W. D. De Doncker,"Doubly fed induction generator system for wind turbines,"IEEE Ind. Appl. Mag., vol. 8, no. 3, pp. 26–33, May 2002.

[2] J. Hu, H. Nian, H. Xu, and Y. He,"Dynamic modeling and improved control of DFIG under distorted grid voltage conditions,"IEEE Trans. Energy Convers., vol. 26, no. 1, pp. 163–175, Mar. 2011.

[3] M. Mohseni, M. S. M. Islam, and M. A. Masoum,"Enhanced hysteresisbased current regulators in vector control of DFIG wind turbine,"IEEE Trans. Power Electron., vol. 26, no. 1, pp. 223–234, Jan. 2011.

[4] H. Polinder, F. F. A. Van der Pijl, G. J. de Vilder, and P. J. Tavner, "Comparison of direct-drive and geared generator concepts for wind turbines," IEEE Trans. Energy Convers., vol. 3, no. 21, pp. 725–733, Sep. 2006.

[5] T. F. Chan and L. L. Lai, "Permanent-magnet machines for distributed generation: A review,"IEEE Power Engg. Annual Meeting, Tampa, FL, USA, Jun. 24–28, 2007, pp. 1–6.

[6] M. E. Haque, M. Negnevitsky, and K. M. Muttaqi,"A novel control strategy for a variable-speed wind turbine with a permanent-magnet synchronous generator," IEEE Trans. Ind. Appl., vol. 46, no. 1, pp. 331–339, Jan./Feb. 2010.

[7] R. Esmali and L. Xu,"Sensorless control of permanent magnet generator in wind turbine application,"IEEE Industry Applications Society Annual Meeting, Tampa, FL, USA, Oct. 8–12, 2006, pp. 2070–2075.

[8] M. Chinchilla, S. Arnaltes, and J. C. Burgos,"Control of permanent-magnet generators applied to variable-speed wind-energy systems connected to the grid,"IEEE Trans. Energy Convers., vol. 21, no. 1, pp. 130–135, Mar. 2006.

[9] S. M. Deghan, M. Mohamadian, and A. Y. Varjani,"A new variable-speed wind energy conversion system using permanent-magnet synchronous generator and Z-source inverter,"IEEE Trans. Energy Convers., vol. 24, no. 3, pp. 714–724, Sep. 2009.

[10] S. Morimoto, H. Nakayama, M. Sanada, and Y. Takeda,"Sensorless output maximization control for

variable-speed wind generation system using IPMSG,"IEEE Trans. Ind. Appl., vol. 41, no. 1, pp. 60–67, Jan./Feb. 2005.

[11] W. Qiao, L. Qu, and R. G. Harley,"Control of IPM synchronous generator for maximum wind power generation considering magnetic saturation," IEEE Trans. Ind. Appl., vol. 45, no. 3, pp. 1095–1105, May/Jun. 2009.

[12] C. N. Bhende, S. Mishra, and S. G. Malla,"Permanent magnet synchronous generator based standalone wind energy supply system," IEEE Trans. Sustain. Energy, vol. 2, no. 4, pp. 361–373, Oct. 2011.

[13] S. M. R. Kazmi, H. Goto, H. J. Guo, and O. Ichinokura,"A novel algorithm for fast and efficient speed-sensorless maximum power point tracking in wind energy conversion systems,"IEEE Trans. Ind. Electron., vol. 58, no. 1, pp. 29–36, Jan. 2011.

[14] S. Zhang, K. J. Tseng, D. M. Vilathgamuwa, T. D. Nguyen, and X. Y. Wang, "Design of a robust grid interface system for PMSG-based wind turbine generators," IEEE Trans. Ind. Electron., vol. 58, no. 1, pp. 316–328, Jan. 2011.

[15] A. Uehara, A. Pratap, T. Goya, T. Senjyu, A. Yona, N. Urasaki, and T. Funabashi,"A coordinated control method to smooth wind power fluctuation of a PMSG-based WECS," IEEE Trans. Energy Convers., vol. 26, no. 2, pp. 550–558, Jun. 2011.

[16] K. Nishida, T. Ahmed, and M. Nakaoka,"A cost-effective high-efficiency power conditioner with simple MPPT control algorithm for wind-power grid integration,"IEEE Trans. Ind. Appl., vol. 47, no. 2, pp. 893–900, Mar. 2011.

[17] M. F. Rahman, L. Zhong, and K. W. Lim, "A direct torque controlled interior permanent magnet synchronous motor drive incorporating field weakening," IEEE Trans. Ind. Appl., vol. 34, no. 6, pp. 1246–1253, Nov. 1998.

[18] I. Takahashi and T. Noguchi,"A new quick response and high efficiency control strategy of an induction motor,"IEEE Trans. Ind. Appl., vol. IA-22, no. 5, pp. 820–827, Sep. 1986.

[19] I. Takahashi and Y. Ohmori,"High-performance direct torque control of an induction motor,"IEEE Trans. Ind. Appl., vol. 25, no. 2, pp. 257–264, Mar./ Apr. 1989.

[20] L. Zhong, M. F. Rahman, and K. W. Lim,"Analysis of direct torque control in permanent magnet synchronous motor drives," IEEE Trans. Power Electron., vol. 12, no. 3, pp. 528–536, May 1997.

[21] M. F. Rahman, L. Zhong, M. E. Haque, and M. A. Rahman,"A direct torque controlled interior permanent magnet synchronous motor drive without a speed sensor,"IEEE Trans. Energy Convers., vol. 18, no. 1, pp. 17–22, Mar. 2003.

[22] L. Tang, L. Zhong, M. F. Rahman, and Y. Hu,"A novel direct torque control for interior permanent magnet synchronous machine drive system with low ripple in flux and torque andfixed switching frequency,"IEEE Trans. Power Electron., vol. 19, no. 2, pp. 346–354, Mar. 2004.

[23] P. C. Krause, O. Wasynczuk, and S. D. Sudhoff, Analysis of Electrical Machinery and Drive System.Piscataway, NJ, USA: IEEE Press, 2002.

[24] M. E. Haque and M. F. Rahman,Permanent Magnet Synchronous Motor Drives: Analysis, Modeling and Control.Germany: VDM Verlag, 2009.

[25] H. Zhu, X. Xiao, and Y. Li,"Torque ripple reduction of the torque predictive control scheme for permanent-magnet synchronous motors,"IEEE Trans. Ind. Electron., vol. 59, no. 2, pp. 871–877, Feb. 2012.

[26] Z. Q. Zhu and J. H. Leong,"Analysis and mitigation of torsional vibration of PM brushless ac/dc

ISSN No: 2348-4845
International Journal & Magazine of Engineering, Technology, Management and Research
A Peer Reviewed Open Access International Journal

drives with direct torque controller,"IEEE Trans. Ind. Appl., vol. 48, no. 4, pp. 1296–1305, Jul./Aug. 2012.

Author Details

Cheerala Sreenivasulu
M.Tech Student
P.V.K.K Institute of Technology.